3262 *Chem. Mater.* **2009,** *21,* 3262–3269
DOI:10.1021/cm9007798

CHEMISTRY OF MATERIALS
Article

Thiophene/Phenylene/Thiophene-Based Low-Bandgap Conjugated Polymers for Efficient Near-Infrared Photovoltaic Applications

Chao-Ying Yu,[†] Chih-Ping Chen,*[,†] Shu-Hua Chan[†,‡] Gue-Wuu Hwang,[†] and Ching Ting*[,†]

[†]*Material and Chemical Laboratories, Industrial Technology Research Institute, Hsiu-Chu 31040, Taiwan, ROC, and* [‡]*Department of Chemical Engineering, National Tsing Hua University, Hsin-Chu 30013, Taiwan*

Received March 20, 2009. Revised Manuscript Received May 24, 2009

We have prepared thiophene/phenylene/thiophene (TPT)-based low bandgap conjugated polymers exhibiting tunable energy levels and investigated their application in solar cells. By incorporating various electron-withdrawing comonomers through Stille coupling reactions, we obtained TPT-based donor/acceptor copolymers having bandgaps ranging from 1.0 to 1.8 eV. We compared the absorption spectra, electrochemistry, field effect hole mobility, and photovoltaic properties of these low bandgap TPT derivatives with those of poly(3-hexylthiophene) (P3HT). The absorption coefficients of the thin films fell in the range from 0.77×10^5 to 1.4×10^5 cm^{-1}. These materials displayed sufficiently high hole mobilities ($> 10^{-3}$ cm^2 V^{-1} s^{-1}) for efficient charge extraction and good fill-factors for organic photovoltaic applications. Electrochemical studies indicated desirable HOMO/LUMO levels, with a good correlation between the HOMO energy levels and the open circuit voltage (V_{oc}) when the polymers were blended with fullerene derivative as an electron acceptor. Power conversion efficiencies of up to 4.3% were achieved under AM 1.5G simulated solar light (100 mW cm^{-2}). Our findings suggest that TPT derivatives presenting suitable electron-withdrawing groups are promising photovoltaic materials.

1. Introduction

In the past decade, organic photovoltaics (OPVs) have attracted considerable attention because they have shown promising potential applications as a result of their low cost, high rates of processing in solution, and flexibility.[1−3] The OPVs with processing into large area[4−7] and device stability [8] of devices were also widely investigated toward commercial application. To obtain higher cell efficiencies, it will be necessary to develop new semiconducting polymers exhibiting high absorption coefficients and broader solar absorptions.[9] Extending the energy bandgap (E_g) to 1000 nm will allow 53% of the available photons to be absorbed, providing a considerable gain in photocurrent. [9] From this point of view, there is interest in developing low bandgap (LBG) conjugated polymers for light harvesting up to longer wavelengths. Nevertheless, an increase in power conversion efficiency (PCE) does not solely rely upon an improved current density—a high open circuit voltage (V_{oc}) and a reasonable fill factor (FF) are also required. The inefficient performance of LBG polymers is often associated with their lower hole mobilities, unwanted highest occupied molecular orbital (HOMO)/lowest unoccupied molecular orbital (LUMO) energy levels, or poor solubilities.[9−11] Recently, some advanced LBG conjugated polymers have exhibited PCEs of greater than 4% under AM 1.5G irradiation at 100 mW cm^{-2}.[12−15] Poly[2,6-(4,4-bis-[2-ethylhexyl]-4*H*-cyclopenta[2,1-*b*;3,4-*b*]-dithiophene)-*alt*-4,7-(2,1,3-benzothiadiazole)] (**PCPDTBT**)[15] and its silole-containing derivatives,[12] which exhibit improved light harvesting in the near-infrared (NIR) region, are at present the most efficient LBG OPV materials, displaying PCEs of 5.5%. Because **PCPDTBT** absorbs more sunlight in the range 380−900 nm, the short circuit density (J_{sc}) of its devices reaches 16 mA cm^{-2} accompanied with reasonable values of V_{oc} and FF. Thus, to maximize the PCE in OPV devices, the active layer material must possess several

*Corresponding author. E-mail: chihping_chen@itri.org.tw, cting@itri.org.tw. Tel: 886-35-913588. Fax: 886-35-827694.

(1) Gunes, S.; Neugebauer, H. S.; Sariciftci, N. S. *Chem. Rev.* **2007**, 107, 1324.
(2) Kim, J. Y.; Lee, K.; Coates, N. E.; Moses, D.; Nguyen, T.-Q.; Dante, M.; Heeger, A. J. *Science* **2007**, 317, 222.
(3) Thompson, B. C.; Fréchet, J. M. J. *Angew. Chem., Int. Ed.* **2008**, 47, 58.
(4) Krebs, F. C.; Jørgensen, M.; Norrman, K.; Hagemann, O.; Alstrup, J.; Nielsen, T. D.; Fyenbo, J.; Larsen, K.; Kristensen, J. *Sol. Energy Mater. Sol. Cells* **2009**, 93, 422.
(5) Krebs, F. C. *Sol. Energy Mater. Sol. Cells* **2009**, 93, 465.
(6) Blankenburg, L.; Schultheis, K.; Schache, H.; Sensfuss, S.; Schrödner, M. *Sol. Energy Mater. Sol. Cells* **2009**, 93, 476.
(7) Niggemanna, M.; Zimmermann, B.; Haschkea, J.; Glatthaar, M.; Gombert, A. *Thin Solid Films* **2008**, 516, 7181.
(8) Jørgensen, M.; Norrman, K.; Krebs, F. C. *Sol. Energy Mater. Sol. Cells* **2008**, 92, 686.
(9) Bundgaard, E.; Krebs, F. C. *Sol. Energy Mater. Sol. Cells* **2007**, 91, 954.
(10) Bundgaard, E.; Krebs, F. C. *Macromolecules* **2006**, 39, 2823.
(11) Bundgaard, E.; Krebs, F. C. *Sol. Energy Mater. Sol. Cells* **2007**, 91, 1019.
(12) Hou, J.; Chen, H.-Y.; Zhang, S.; Li, G.; Yang, Y. *J. Am. Chem. Soc.* **2008**, 130, 16144.
(13) Chen, C.-P.; Chan, S.-H.; Chao, T.-C.; Ting, C.; Ko, B.-T. *J. Am. Chem. Soc.* **2008**, 130, 12828.
(14) Wienk, M. M.; Turbiez, M.; Gilot, J.; Jannsen, R. A. *J. Adv. Mater.* **2008**, 20, 2556.
(15) Peet, J.; Kim, J. Y.; Coates, N. E.; Ma, W. L.; Moses, D.; Heeger, A. J.; Bazan, G. C. *Nat. Mater.* **2007**, 6, 497.

 Published on Web 06/29/2009

Scheme 1. Structure and Synthesis of the TPT-Based Copolymers

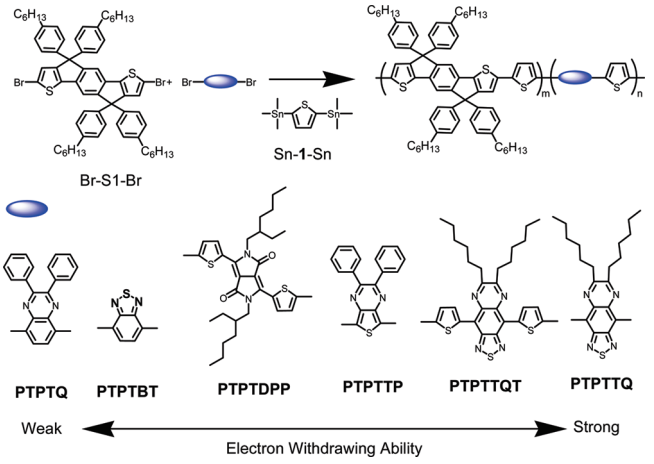

factors: superior solar harvesting, desirable HOMO/LUMO energy levels for a large V_{oc} when blended with fullerene derivatives, and high mobilities for effective carrier transport to provide a reasonable FF.[16]

To design new semiconducting polymers for OPV applications, we investigate the behaviors of a series of thiophene/phenylene/thiophene (TPT) derivatives.[13,17] The TPT unit is a superior building block for conjugated polymers because of its forced coplanarity. The use of tetrahexylaryl groups, positioned as peripheral substituents of the TPT units, tailors the intermolecular interactions between the polymer chains to provide improved morphologies and processability (**S1**; Scheme 1). Moreover, poly(TPT) derivatives possess high field-effect hole mobilities (up to 10^{-3} cm^2 V^{-1} s^{-1}); when blended with fullerene-based acceptors, they have provided a promising PSC performance of up to 4.3%.[13] In addition, TPT-based devices exhibit impressively large values of V_{oc} (>0.8 V) and reasonable FFs (>0.5). Our goal in this study was to develop new TPT derivatives to extend the absorption wavelength to the NIR region to provide higher current output. One of the most promising strategies to tailor the energy levels of conjugated polymers is via the donor/acceptor route, in which electron-deficient heterocycles (e.g., benzothiadiazole, quinoxaline, pyrazine, oxazole) are alternated with aromatic electron-rich rings (e.g., phenylene, thiophene, pyrrole) to prepare low-bandgap polymers.[1,9] Scheme 1 illustrates how the incorporation of strong electron-withdrawing moieties provides LBG polymers exhibiting a range of optoelectronic characteristics. The interaction between the electron-rich donors and electron-deficient acceptors has resulted in new polymers exhibiting bandgaps ranging from 1 to 1.9 eV. Thus, we have studied the effects of the acceptor strength and structural coplanarity on the optical and electrochemical properties, obtained the field-effect carrier mobility from the thin film transistor (TFT) devices, and correlated it to the polymer structures. These new LBG TPT polymers display high-performance PSC characteristics, with the PCEs of the **PTPTQ**-, **PTPTBT**-, and **PTPTDPP**-based devices reaching 4.2%.

2. Experimental Section

Materials and Equipment for Polymer Solar Cells. All chemicals were purchased from Aldrich and used as received unless otherwise specified. ^{1}H NMR (500 MHz) spectra were recorded using a Bruker spectrometer. Absorption spectra were recorded on a Perkin−Elmer Lambda 950 UV−vis spectrophotometer. The molecular weights of the polymers were measured using the GPC method with polystyrene standards. The morphologies of the polymer films were analyzed using a VEECO DICP-II atomic force microscope operated in the dynamic force mode at ambient temperature and an etched Si probe operated under a resonant frequency of 131 kHz and a spring constant of 11 N m^{-1}. CV traces were recorded using an Autolab PGSTAT302 operated at a scan rate of 50 mV s^{-1}, equipped with Pt electrodes and a Ag/Ag$^+$ (0.10 M $AgNO_3$ in MeCN) reference electrode in an anhydrous, N_2-saturated solution of 0.1 M Bu_4NClO_4 in MeCN. Bu_4NClO_4 (98%, TCI) was recrystallized three times from methanol/water (1:1) and then dried at 100 °C under reduced pressure. A Pt plate coated with a thin polymer film was used as the working electrode; a Pt wire and a Ag/Ag$^+$ electrode were used as the counter and reference electrodes, respectively. The electrochemical potential was calibrated against Fc/Fc$^+$. $I-V$ curves of the PSC devices were measured using a computer-controlled Keithley 2400 source measurement unit (SMU) equipped with a Peccell solar simulator under AM 1.5G illumination (100 mW cm^{-2}). The illumination intensity was calibrated using a standard Si photodiode detector equipped with a KG-5 filter. The output photocurrent was adjusted to match the photocurrent of the Si reference cell to obtain a power density of 100 mW cm^{-2}. The efficiency of 3.5% of a P3HT/PCBM reference cell measured under illumination in our laboratory was verified to be 3.4% under AM1.5G conditions (100 mW cm^{-2}) in National Institute of Advanced Industrial Science and Technology (AIST, Japan). After encapsulation, all device measurements were operated in an ambient atmosphere at 25 °C. Bottom-contact geometry was used to fabricate the thin film FETs. A thermal oxide layer having a thickness of 120 nm was grown in a furnace on an N^{2+}-type low-resistance wafer, which acted as a common gate electrode. Pt metal was used for the source and drain electrodes, which were defined using photolithography. The devices had a channel width of 1000 μm and a channel length of 10 μm. Thin films of polymers were prepared by spin-coating a 1.0 wt % $CHCl_3$ or *o*-DCB solution onto a modified SiO_2 surface and then drying for 1 h on a hot plate at 150 °C under vacuum. Electronic measurements were performed at room temperature in air by using semiconductor parameter analyzer (4156C, Agilent).

Synthesis. *Polymer PTPTQ*. Tris(dibenzylideneacetone)dipalladium(0) (5.5 mg) and tri(*o*-tolyl)phosphine (14.6 mg) were added to a mixture of 5,8-dibromo-2,3-diphenylquinoxaline (110 mg, 0.25 mmol), TPT (266 mg, 0.25 mmol), and 2,5-bis(trimethylstannyl)thiophene (205 mg, 0.5 mmol) in dry chlorobenzene (5 mL). The reaction mixture was purged with N_2 and subjected to three freeze/pump/thaw cycle to remove O_2. The mixture was heated in a microwave reactor for 30 min. The dark solution was poured into methanol (1 L), and the

(16) Zhu, Z.; Waller, D.; Gaudiana, R.; Morana, M.; Muhlbacher, D.; Scharber, M.; Brabec, C. *Macromolecules* **2007**, 40, 1981.
(17) Chan, S.-H.; Chen, C.-P.; Chao, T.-C.; Ting, C.; Ko, B.-T. *Macromolecules* **2008**, 41, 5519.

black precipitate was collected on a membrane filter. The polymer was washed for 72 h through Soxhlet extraction with methanol, acetone, and hexane sequentially; the soluble fraction was then collected through extraction with $CHCl_3$. The extract was concentrated and precipitated into methanol to yield the polymer as a deep-red product (70%). GPC (THF): M_w = 62 400 g mol^{-1}; λ_{max} = 550 nm. ^{1}H NMR ($CDCl_3$, 500 MHz): δ 7.78−7.71 (br, 2H), 7.23−6.95 (br, 32H), 2.55 (t, 8H), 1.55 (m, 8H), 1.27 (br, 24H), 0.84 (t, 12H). Other polymers were prepared in analogous fashion.

Polymer PTPTBT. Deep-red solid (65%). GPC (THF): M_w = 38,600 g mol^{-1}; λ_{max} = 570 nm. ^{1}H NMR ($CDCl_3$, 500 MHz) δ:7.85−8.25 (br, 2H), 7.50−7.00 (br, 24H), 2.56 (t, 8H), 1.65 (m, 8H), 1.30 (br, 24H), 0.86 (t, 12H).

Polymer PTPTTP. Dark-green solid (75%). GPC (THF): M_w = 32,400 g mol^{-1}; λ_{max} = 510 nm. ^{1}H NMR ($CDCl_3$, 500 MHz) δ: 7.60−7.07 (br, 32H), 2.57 (t, 8H), 1.68 (m, 8H), 1.30 (br, 24H), 0.88 (t, 12H).

Polymer PTPTDPP. Black solid (72%). GPC (THF): M_w = 51,900 g mol^{-1}; λ_{max} = 706 nm. ^{1}H NMR ($CDCl_3$, 500 MHz) δ: 8.96 (d, 2H), 7.46−7.09 (br, 26H), 4.09 (d, 4H), 2.57 (t, 8H), 1.90 (m, 2H), 1.59−1.26 (br, 48H), 0.88 (br, 24H).

Polymer PTPTTQT. Black solid (40%). GPC (THF): M_w = 36,800 g mol^{-1}; λ_{max} = 495 nm. ^{1}H NMR (*o*-$C_6D_4Cl_2$, 500 MHz) δ: 9.43 (d, 2H), 7.89−6.91 (br, 26H), 3.29 (t, 4H), 2.65 (t, 8H), 2.40 (m, 4H), 164−1.30 (br, 44H), 0.95 (br, 18H).

Polymer PTPTTQ. Black solid (57%). GPC (THF): M_w = 23,300 g mol^{-1}; λ_{max} = 490 nm. ^{1}H NMR ($CDCl_3$, 500 MHz) δ: 9.09 (d, 2H), 7.10−7.46 (br, 22H), 3.17 (t, 4H), 2.59 (t, 8H), 2.10 (m, 4H), 161−1.26 (br, 44H), 0.89−0.76 (br, 18H).

Photovoltaic Cell Fabrication and Testing. All bulk-heterojunction PV cells were prepared using the following device fabrication procedure.[13] Glass/indium tin oxide (ITO) substrates [Sanyo, Japan (8 Ω/□)] were sequentially patterned lithographically, cleaned with detergent, ultrasonicated in acetone and isopropyl alcohol, dried on a hot plate at 120 °C for 5 min, and treated with oxygen plasma for 5 min. Poly(3,4-ethylene-dioxythiophene):poly(styrene-sulfonate) (PEDOT:PSS, Baytron P-VP AI4083) was passed through a 0.45-μm filter prior to being deposited on ITO at a thickness of ca. 30 nm through spin-coating at 3000 rpm in air; the sample was then dried at 150 °C for 30 min inside a glovebox. A blend of 1-(3-methoxycarbonyl)propyl-1-phenyl-[6,6]-C_{71} ($PC_{71}BM$) and the polymer [3:1 (w/w), 7.5 mg mL^{-1} in *o*-DCB] was stirred overnight in *o*-DCB, filtered through a 0.2-μm poly(tetrafluoroethylene) (PTFE) filter, and then spin-coated (500−1000 rpm, 30 s) on top of the PEDOT:PSS layer. The device was completed by depositing a 30-nm-thick layer of Ca and a 100-nm-thick layer of Al at pressures of less than 10^{-6} torr. The active area of the device was 4 mm^2. Finally the cell was encapsulated using UV-curing glue (Nagase, Japan).

3. Results and Discussion

3.1. Synthesis of LBG Conjugated Polymers. Recently, we described the synthesis of poly(TPT) derivatives for use as OPV materials.[13,17] In this present study, we adopted the donor/acceptor approach to develop LBG polymers possessing various bandgap structures. The interactions between a strong electron donor (D) and a strong electron acceptor (A) lead to increased double bond character between these units, thereby decreasing the bandgap of polymers. Therefore, changing the electron-withdrawing moieties allows further tuning of the polymer's optoelectronic properties. We used Pd(0)-catalyzed Stille coupling in chlorobenzene under microwave heating to synthesize copolymers consisting of thiophene (**1**) and TPT moieties as electron-donating units and a variety of electron-accepting moieties (Scheme 1). We first synthesized comonomers displaying a range of electron-withdrawing abilities, namely, 5,8-dibromo-2,3-diphenylquinoxaline (**Q**),[18] 2,1,3-benzothiadiazole (**BT**), 3,6-bis(5-bromothiophen-2-yl)-2,5-bis(2-ethylhexyl)pyrrolo[3,4-*c*]pyrrole-1,4-dione (**DPP**),[14,19] 5,7-dibromo-2,3-diphenylthieno[3,4-*b*]pyrazine (**TP**),[20] 4,9-bis(5-bromothiophen-2-yl)-6,7-dihexyl[1,2,5]thiadiazolo[3,4-*g*]quinoxalines (**TQT**),[21,22] and 4,9-dibromo-6,7-dihexyl[1,2,5]thiadiazolo[3,4-*g*]quinoxalines (**TQ**) according to previous reports[18−22] and used them to tune the bandgap of the polymers. Herein, we use the descriptor **PTPTXXX** to identify each of these TPT-based conjugated polymers, with the characters **XXX** denoting the electron-withdrawing moiety. Figure 1 presents the ^{1}H NMR spectra of **PTPTQ**, **PTPTDPP**, and **PTPTTQ**. The peaks at δ 7.6−8.2 ppm in Figure 1a represent the resonances of the protons of the **Q** unit. We assign the characteristic signals at δ 7.50−7.00 ppm to the resonances of protons on the thiophene ring, phenylene ring, and protons on phenyl side groups of the TPT unit. The peak at δ 2.55 ppm represents the methylene group attached to the phenyl group of the TPT unit. The peaks in the range δ 1.60−0.88 ppm arise from the tetrahexyl substituents of the TPT unit. In the spectrum of **PTPTDPP** (Figure 1b), we assign the peaks at δ 8.9, 4.1, and 1.9 ppm to the resonances of the protons of the thiophene, methylene, and methine groups, respectively, of the **DPP** unit. In the spectrum of **PTPTTQ** (Figure 1c), the peaks at δ 9.1, 3.2, and 2.1 ppm are the resonances of the protons of the thiophene unit adjacent to the **TQ** moiety and that of the pendent methylene groups of the **TQ** unit, respectively. We characterized the weight-average molecular weights (M_w) and polydispersity indexes (PDIs, M_w/M_n) using gel permeation chromatography (GPC) with THF as the eluent and polystyrenes as internal standards. All of the polymers were readily soluble in THF, except for **PTPTTQT** and **PTPTTQ**, which were only moderately soluble after ultrasonication at high temperature (70 °C). Table 1 lists the values of M_w and PDI of our polymers. Each of these materials possessed good thermal stability [5% weight-loss temperature (T_d) > 410 °C] as indicated by thermogravimetric analysis (TGA). When investigating the thermal behavior of these polymers using differential scanning calorimetry (DSC), we observed no clear thermal transitions in the temperature range from 40 to 300 °C.

3.2. Optical Properties. We prepared high-quality films of **PTPTQ**, **PTPTBT**, **PTPTDPP**, and **PTPTTP** through spin-coating of the polymers from chloroform

(18) Chen, C. T.; Wei, Y.; Lin, J. S.; Moturu, M. V. R. K.; Chao, W. S.; Tao, Y. T.; Chien, C. H. *J. Am. Chem. Soc.* **2006**, 128, 10992.
(19) Horn, M.; Hepuzer, Y.; Yagci, Y.; Eran, B. B.; Harabagiu, U. C. V.; Pinteala, M.; Simionescu, B. C. *Eur. Polym. J.* **2002**, 38, 2197.
(20) Shahid, M.; Ashraf, R. S.; Klemm, E.; Sensfuss, S. *Macromolecules* **2006**, 39, 7844.
(21) Kitamura, C.; Tanaka, S.; Yamashita, Y. *Chem. Mater.* **1996**, 8, 570.
(22) Uno, T.; Takagi, K.; Tomoeda, M. *Chem. Pharm. Bull.* **1980**, 28, 1909.

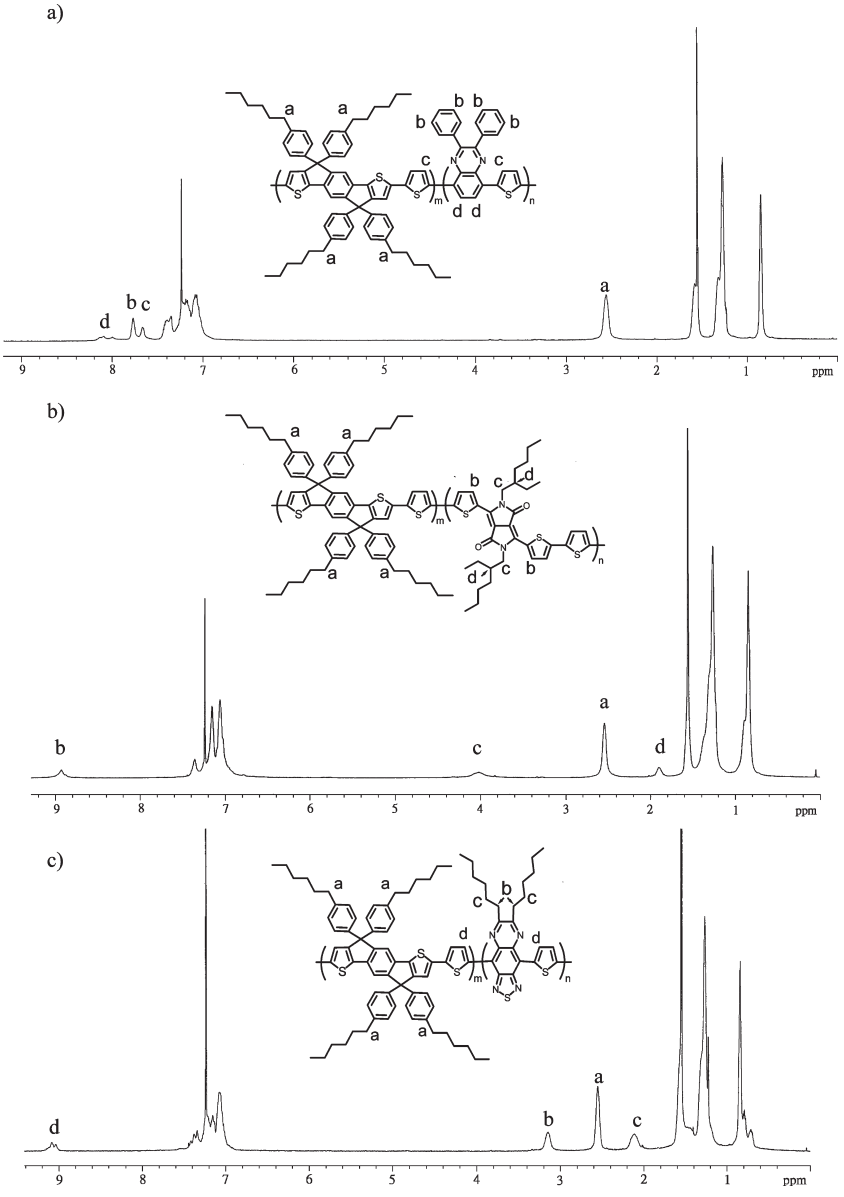

Figure 1. ^{1}H NMR spectra of (a) PTPTQ, (b) PTPTDPP, and (c) PTPTTQ.

Table 1. Molecular Weights, OTFT Mobilities, and Optical and Redox Properties of Various Polymers

	M_w (PDI)	T_d[a] (°C)	λ_{max}	α[b]	E_g^{opt} (eV)	HOMO (eV)	LUMO (eV)	μ_h (cm^2 V^{-1} s^{-1})	on/off
P3HT	47 000 (2.45)	450	552	1.9	1.9	−5.07	−3.24	6.5×10^{-2}	1.3×10^3
PTPTQ	62 400 (1.52)	490	550	1.34	1.8	−5.30	−3.37	3.3×10^{-3}	2.4×10^4
PTPTBT	38 600 (1.74)	514	570	1.4	1.7	−5.3	−3.53	3.4×10^{-3}	5.6×10^6
PTPTDPP	51 900 (1.82)	414	706	1.29	1.4	−5.25	−3.60	2.7×10^{-3}	1.8×10^4
PTPTTP	32 400 (1.61)	440	510	1.22	1.2	−5.03	−3.63	1.1×10^{-3}	1.9×10^3
PTPTTQT	36 800 (2.02)	460	495	1.2	1.2	−5.12	−3.66	8.1×10^{-3}	1.6×10^4
PTPTTQ	23 300 (1.45)	460	490	0.77	1.0	−5.16	−3.67	1.9×10^{-3}	4.6×10^3

[a] 5% weight loss. [b] Absorption coefficient of the solid thin film at λ_{max} ($\times 10^5$ cm^{-1}).

($CHCl_3$), THF, or *o*-dichlorobenzene (*o*-DCB) solution; although **PTPTTQT** and **PTPTTQ** are only moderately soluble in $CHCl_3$, they can be dissolved in *o*-DCB. Therefore, we used DCB as the solvent to obtain optical-quality films of each polymer for device characterization. Figure 2 displays the UV−vis absorption features of the polymer films in the solid state, as well as that of P3HT for comparison; Table 1 summarizes these spectroscopic data. In the presence of stronger electron-withdrawing groups, the bandgap (E_g) of the poly-(TPT) derivatives shifted from 1.8 to 1 eV gradually. Apart from **PTPTQ** and **PTPTBT**, the materials displayed typical D/A LBG polymer characteristics, namely, two absorption bands with maxima at visible and NIR regions arising from the absorbances of the TPT-rich (larger E_g^{opt}) and electron withdrawing group-rich (narrower E_g^{opt}) structures. The values of E_g^{opt} values determined from the onset of absorptions of **PTPTQ**, **PTPTBT**, **PTPTDPP**,

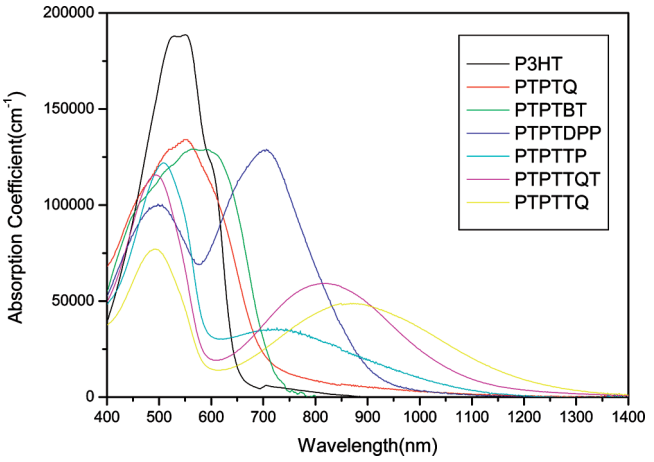

Figure 2. Absorption spectra of **PTPTs** and P3HT films.

PTPTTP, **PTPTTQT**, and **PTPTTQ** were 1.8, 1.7, 1.4, 1.2, 1.2, and 1.0 eV, respectively. Relative to P3HT, a strong red shift in the absorption edge—from 650 to 1240 nm—was obtained after introducing the **TQ** group. The smaller values of E_g of these copolymers, compared with those we reported previously, are due to intramolecular charge transfer (ICT) between the thiophene moieties and the **Q**, **BT**, **DPP**, **TP**, and **TQ** units. The order of the acceptor strength—**Q** < **BT** < **DPP** < **TP** < **TQ**—is in agreement with a decreasing trend in the values of the optical E_g for these alternative copolymers. A smaller value of E_g should improve light harvesting and, therefore, enhance the photocurrent of the devices. Generally, the amount of absorbed light depends not only on the wavelength at the edge of the absorption but also on the intensity of the absorption. As indicated in Figure 2, the thin films of **PTPTQ** (1.34×10^5 cm^{-1} at λ_{max} = ca. 550 nm), **PTPTBT** (1.40×10^5 cm^{-1} at λ_{max} = ca. 570 nm), and **PTPTDPP** (1.29×10^5 cm^{-1} at λ_{max} = ca. 706 nm) display high absorption coefficients (Table 1), comparable with that of P3HT film (1.9×10^5 cm^{-1} at λ_{max} = ca. 552 nm). The absorption coefficients at λ_{max} for **PTPTTP**, **PTPTTQT**, and **PTPTTQ** are all relatively low.

3.3. Electrochemical Properties. We recorded cyclic voltammograms (CVs) using an Autolab PGSTAT302 instrument operated at a scan rate of 50 mV s^{-1}, while equipped with Pt electrodes and a Ag/Ag$^+$ (0.10 M of $AgNO_3$ in MeCN) reference electrode in an anhydrous, N_2-saturated solution of 0.1 M tetrabutylammonium perchlorate (Bu_4NClO_4) in MeCN. Table 1 and Figure 3 summarize the CV data of our TPT-based copolymers. We calculated the HOMO energy level using the equation

$$\text{HOMO} = -[E_{ox} - E_{1/2}(\text{ferrocene}) + 4.8]\ \text{V}$$

where E_{ox} is the onset oxidation potential vs SCE. We estimated the LUMO energy levels from the values of E_{red} by using the equation

$$\text{LUMO} = -[E_{red} - E_{1/2}(\text{ferrocene}) + 4.8]\ \text{V}$$

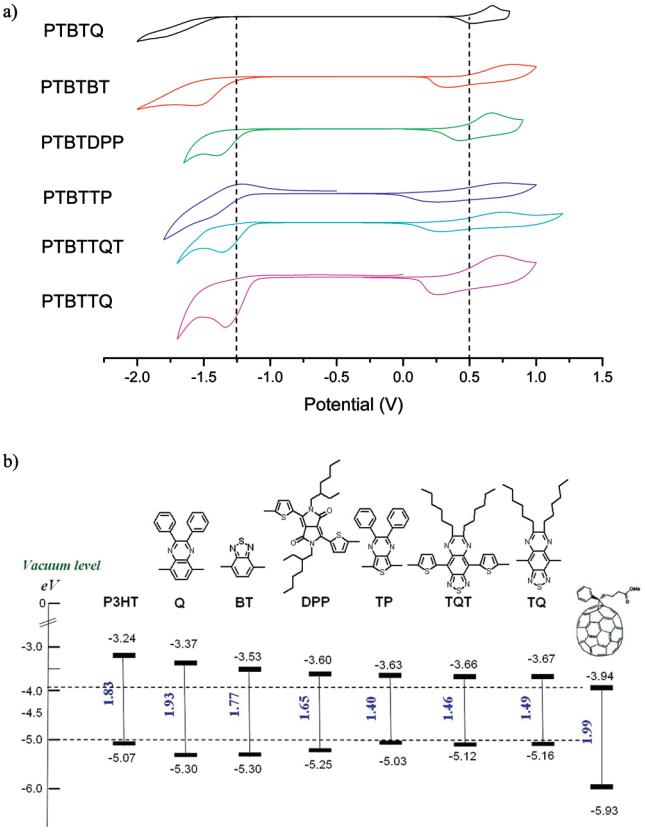

Figure 3. (a) Cyclic voltammograms of TPT based copolymers. (b) Energy-level diagram showing the HOMO and LUMO energy levels of **PTPTs**, P3HT, and $PC_{71}BM$.

Note that because of the change of electrolyte for the CV measurements, the HOMO and LUMO energy levels of **PTPTBT** are slightly different from those reported previously.[13] The LUMO energy level of PCBM has been reported to have values ranging between −3.7 and −4.3 eV due to the uncertainties in measurement. In our hands, using the same procedures, we determined the LUMO and HOMO energy levels of PCBM to be −3.94 and −5.93 eV, respectively. The corresponding HOMO energy levels of **PTPTQ**, **PTPTBT**, **PTPTDPP**, **PTPTTP**, **PTPTTQT**, and **PTPTTQ** are −5.30, −5.30, −5.25, −5.03, −5.12, and −5.16 eV, respectively; their LUMO energy levels are −3.37, −3.53, −3.60, −3.63, −3.66, and −3.67 eV, respectively. From these values, the electrochemical bandgaps (E_g^{ec}) for each compound can be determined. The E_g^{ec} values of our TPT-based copolymers are systematically larger than their values of E_g^{opt}. Figure 3b presents the resulting energy band diagram in relation to the relative energy levels of the acceptor ($PC_{71}BM$) used in this study and those of P3HT. According to band theory, the molecular highest occupied band, which originates from the molecular orbital hybridization of the energy levels of the donor and the acceptor moieties, results in D−A systems exhibiting varius values of E_g and HOMO/LUMO energy levels.[23] Typically, the introduction of electron withdrawing groups reduces E_g by lowering the LUMO energy levels, and the introduction of electron donating groups reduces E_g by raising the HOMO

(23) Roncali, J. *Chem. Rev.* **1997**, 97, 173.

Table 2. Characteristic *I*−*V* Parameters from Device Testing under Standard AM 1.5G Conditions

	J_{sc} (mA cm^{-2})	V_{oc} (V)	FF	η (%)[c]
P3HT[a]	9.9	0.64	0.62	3.9
PTPTQ[b]	9	0.81	0.57	4.2
PTPTBT[b]	10.1	0.8	0.53	4.3
PTPTDPP[b]	10.3	0.75	0.54	4.2
PTPTTP[b]	1.94	0.51	0.41	0.40
PTPTTQT[b]	3.6	0.54	0.43	0.84
PTPTTQ[b]	2.57	0.54	0.36	0.50

[a] Using $PC_{61}BM$ (purchased from Nano-C) as the acceptor (P3HT:$PC_{61}BM$ = 1:1, w/w). [b] Using $PC_{71}BM$ (purchased from Solenne) as the acceptor. [c] Average value of PCE calculated from four pixels in the PSC device.

energy levels.[24] In this study, we found that the incorporating of electron withdrawing groups not only raised the HOMO energy level but also lowered the LUMO because of its random copolymer characteristic. LUMO offsets of the acceptor and donor must be sufficiently large enough to guarantee energetically efficient charge transfer and, therefore, devices exhibiting higher current output. Figure 3b reveals that the LUMO energy levels of our polymers are approximately 0.27−0.57 eV higher than the LUMO energy level of PCBM; this range is a reasonable one for efficient exciton dissociation from polymers. Furthermore, the open circuit voltage (V_{oc}) can be increased by increasing the difference between the HOMO energy levels of the polymers and the LUMO energy level of PCBM.[9] In comparison with P3HT, the extra benefit observed from lower HOMO levels associated with the **PTPTQ**, **PTPTBT**, and **PTPTDPP** is higher values of V_{oc} in the fabricated devices.

3.4. Determining Hole Mobility from Field Effect Transistor Characteristics. Transport properties are important factors affecting OPV performance. To diminish photocurrent loss through recombination, it is generally acknowledged that a carrier mobility of greater than 10^{-3} cm^2 V^{-1} s^{-1} is essential for the donor material.[16] In this study, we determine the field effect carrier mobilities of our copolymers in thin film field effect transistors (FETs).[17] The source−drain current (I_{DS}) as a function of the source−drain voltage (V_{DS}) is measured at gate voltages (V_G) ranging from 0 to −40 V. Transistor behavior was observed when applying a negative V_G, indicating that the fabricated FETs had p-channel characteristics. The field effect hole mobility (μ) was estimated from the saturation regime current of I_{DS}, using the equation

$$I_D = (W/2L)C_0\mu(V_G - V_T)^2$$

where W is the channel width (1000 μm), L is the channel length (10 μm), C_0 is the capacitance per unit area of the gate dielectric layer (SiO_2, 100 nm; C_0 = 34.5 nF cm^{-2}), and V_T is the threshold voltage. We calculated the hole mobilities of copolymers from the transport characteristics of the FETs by plotting $I_D^{1/2}$ with respect to V_G; Table 1 summarizes the results. The

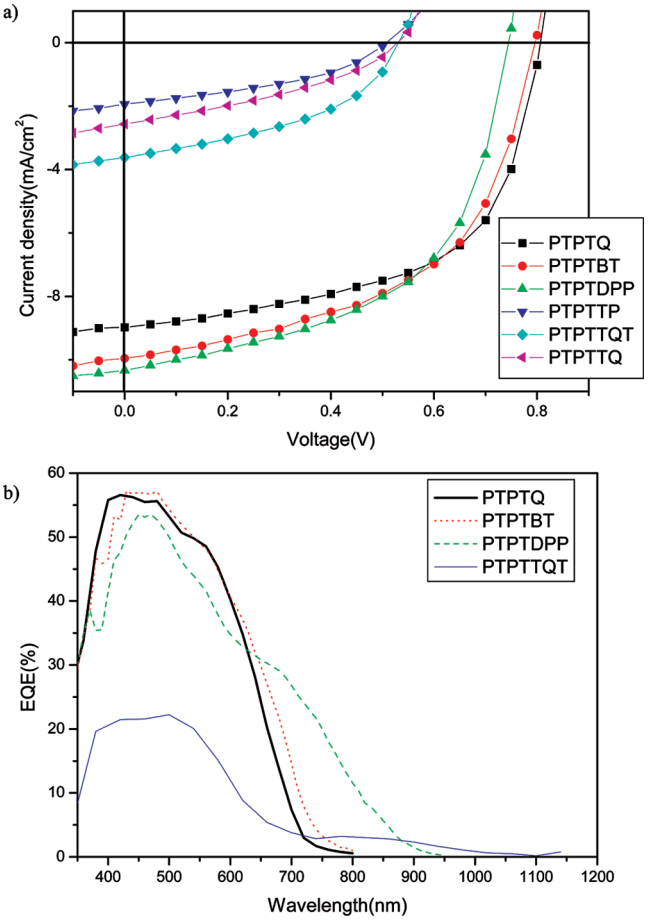

Figure 4. (a) Current density−potential characteristics of TPT-based solar cell devices under illumination with AM 1.5G solar simulated light (100 mW/cm^2). (b) The external quantum efficiency (EQE) spectra of devices fabricated with the **PTPTs**/$PC_{71}BM$ system.

calculated hole mobilities of **PTPTQ**, **PTPTBT**, **PTPTDPP**, **PTPTTP**, **PTPTTQT**, and **PTPTTQ** are 3.3×10^{-3}, 3.4×10^{-3}, 2.7×10^{-3}, 1.1×10^{-3}, 8.1×10^{-3}, and 1.9×10^{-3} cm^2 V^{-1} s^{-1}, respectively. The mobility of P3HT is approximately 5.6×10^{-2} cm^2 V^{-1} s^{-1}, and the on/off ratio is 1.3×10^3 under the same experimental conditions. Although the hole mobilities of our copolymers are not as high as that of P3HT, they are within the desirable range for OPV applications. Their relatively low mobilities may be due to the lack of regioregularity required for good polymer packing. The relatively low on/off current ratio of **PTPTTP** may have resulted from it high-lying HOMO energy level, and thus, ambient oxygen doping of the organic semiconductor leads to a larger off-current. Thus, we suspected that the low HOMO energy levels of other polymers would diminish the possibility of oxygen doping defects in ambient air, thereby providing for good stability.

3.5. Photovoltaic Properties. We fabricated photovoltaic cells by spin-coating the blends from *o*-DCB solutions at various polymer-to-PCBM ratios. The PSCs, which had the layered configuration of glass/ITO/PEDOT:PSS/polymer:PCBM/Ca/Al, were fabricated using established methods.[13,17] The layers of Ca (30 nm) and Al (100 nm) were thermally deposited followed by

(24) Ajayaghosh, A. *Chem. Soc. Rev.* **2003**, 32, 181.

encapsulation with a UV-curing glue. The $I-V$ characteristics were measured in air. The optimal performance of these **TPT**-based devices occurred when using a 6.6 mg mL^{-1} polymer solution in *o*-DCB, a spin-coating rate of 800 rpm for 60 s, and a polymer-to-PCBM ratio of 1:3 (w/w). All devices were tested without thermal annealing. The thickness of the active layer in our cell was ca. 90 nm; it could be controlled by changing both the spin-coating rate and the concentration of the active layer solution. Table 2 summarizes the output characteristics of the **TPT**- and P3HT-based devices. The cell performance of our P3HT-based device is comparable with that reported previously when prepared from a 17 mg mL^{-1} P3HT/$PC_{61}BM$ (1:1, w/w) solution in DCB. Figure 4a displays the $I-V$ characteristics of representative cells prepared from various polymer blends with $PC_{71}BM$. The **PTPTQ**-, **PTPTBT**-, and **PTPTDPP**-based cells display the highest AM1.5G PCEs ($>4.2\%$), which are reproducible (10% variation from five individual PSC devices). The overall PCEs are slightly higher than that of the corresponding P3HT device mainly due to the higher V_{oc} of the **PTPTQ** and **PTPTBT** based devices by approximately 0.16 V, while that of the **PTPTDPP** device was higher by approximately 0.11 V. These higher values of V_{oc} for these copolymer devices are consistent with their lower HOMO energy levels (Figure 3b). While the most successful LBG OPV materials to date are copolymers featuring benzothiadiazole as the acceptor,[12,13,15,25] the performance of **PTPTQ** clearly represents among the highest reported efficiencies for known quinoxaline-based LBG polymers. When comparing the performance of our **PTPTDPP** device with that described in a previous report,[14] our present device exhibits a superior value of V_{oc}, but slightly lower values of J_{sc} and FF. Figure 4b compares the external quantum efficiency (EQE) spectra of the devices fabricated using poly(TPT)/$PC_{71}BM$ materials. The spectral responses of the **PTPTQ** and **PTPTBT** devices reveal significant contributions of the EQE at wavelengths between 350 and 700 nm, with the maximum EQE being approximately 56% at 460 nm. The **PTPTDPP**-based device however, exhibites even better spectral response in the range from 350 to 900 nm, with its maximum EQE being approximately 53%. Convolution of the spectral responses with the photon flux AM 1.5G spectra (100 mW cm^{-2}) provides estimates for the values of J_{sc} under irradiation of the **PTPTQ**-, **PTPTBT**-, and **PTPTDPP**-based devices of 8.4, 8.8, and 9.3 mA cm^{-2}, respectively. Because of a mismatch between the EQE light source and photon flux AM 1.5G, an approximately 10% mismatch exists between the convolution and solar simulator data. The PCEs of the **PTPTTP**-, **PTPTTQT**-, and **PTPTTQT**-based devices are significantly lower in comparison with those of the others, thereby accounting for the remarkable decreases in current density and V_{oc}. The low values of V_{oc} for the **PTPTTP**-, **PTPTTQT**-, and PTPTTQT-based devices can be attributed to their higher HOMO energy levels. The $I-V$ characteristics revealed a good correlation between the HOMO energy levels and the open circuit voltages (V_{oc}). This result highlights the importance of energy levels consideration when designing LBG polymers. In terms of absorption, high photocurrents should be obtained from these polymers because of their NIR absorptions and better spectral matching with the solar spectrum. As indicated in Figure 4b, the spectral response of the **PTPTTQT**-based device featured contributions from the EQE in the wavelength range between 350 and 1100 nm, with the maximum EQE being approximately 20% at 460 nm; it was less than 5% in the range from 700 to 1100 nm. One reason for the significantly lower spectral response is the lower absorption coefficient of these polymers. In addition to desirable absorption and HOMO/LUMO energy levels, the morphology of the blend film also plays an important role. Therefore, we used tapping mode atomic force microscopy (AFM) to investigate the surface morphologies of our blend films. As indicated in Figure S1 (Supporting Information), PTPTQ, **PTPTBT**, and **PTPTDPP** displayed relatively low levels of roughness (<0.8 nm) and no significant aggregation, whereas **PTPTTP**, **PTPTTQT**, and PTPTTQ feature higher degrees of roughness and island-like aggregation. These observations suggest that morphological variations may be another reason for the different device performances. Taken together, our results suggest that LBG polymers must simultaneously possess high mobility and broad utility of sunlight. In addition, desirable HOMO/LUMO energy levels and optimal morphologies of blend films are required for high-performance OPV materials.

The most successful LBG OPV materials to date are copolymers featuring donor−acceptor as design concept, including carbazole, TPT, and thiophene based conjugated polymers.[13−15,25−27] These classes of LBG materials are capable of better harvesting the solar flux, featuring high hole mobilities ($>10^{-3}$ cm^2 V^{-1} s^{-1}) and potentially increasing V_{oc} due to their larger IP. Among them, **PCPDTBT** and poly[*N*-9″-hepta-decanyl-2,7-carbazole-*alt*-5,5-(4′,7′-di-2-thienyl-2′,1′,3′-benzothiadiazole) (**PCDTBT**) represent the most efficient examples with thiophene and carbazole adopting this design concept.[25,26] When comparing the intrinsic properties of our **PTPTBT** with **PCPDTBT** and **PCDTPT** that are listed in previous literatures, the corresponding bandgaps of **PTPTBT**, **PCPDTBT**, and **PCDTPT** are 1.70, 1.45, and 1.98 eV, respectively; their HOMO energy levels are −5.3, −5.3, and −5.5; and their field-effect hole mobilities are 3.4×10^{-3}, 2×10^{-2}, and 1×10^{-3} cm^2 V^{-1} s^{-1}. For the **PCPDTBT** based device, an initial efficiency of 3.2% was achieved[26], and by morphology control using a higher boiling point solvent (1,8-octanedithiol) as additive, the PCE of the device reached 5.5%, with a J_{sc} of 16.2 mA/cm^2, a V_{oc} of 0.62 V, and a FF of 0.55.[15] In the initial

(25) Blouin, N.; Michaud, A.; Leclerc, M. *Adv. Mater.* **2007**, 19, 2595.
(26) Mühlbacher, D.; Scharber, M.; Morana, M.; Zhu, Z.; Waller, D.; Gaudiana, R.; Brabec, C. *Adv. Mater.* **2006**, 18, 2884.
(27) Park, S. H.; Roy1, A.; Beaupré, S.; Cho, S.; Coates, N.; Moon, J. S.; Moses, D.; Leclerc, M.; Lee, K.; Heeger, A. J *Nature Photonics* **2009**, 3, 297.

report of the **PCDTBT**, Leclerc and colleagues demonstrated a device PCE of 3.6%.[25] A combination of optical spacer and morphology controlled protocols, PCE up to 6.1% with a J_{sc} of 10.6 mA/cm^2, a V_{oc} of 0.88 V, and a FF of 0.66 for **PCDTBT**, was obtained.[27] In comparison with **PCPDTBT**-, **PCDTPT**-, and **PTPTBT**-based devices, **PCPDTBT** shows significant enhanced photocurrent due to its lower bandgap property. Higher mobility of **PCPDTBT** allows a thicker active layer (110 nm) to harvest more solar spectrum. (Optimal film thicknesses of PCPTPT and PTPTBT in their devices are around 90 nm.) **PCDTBT** device shows better V_{oc} due to its deeper HOMO level and exhibits the best performance of the OPV system studied to date. Taken together, for new synthesized conjugated polymers, the ability to control the morphology and device engineering is critical to further optimizing its efficiency.

4. Conclusion

We have synthesized soluble TPT-based copolymers through Stille coupling polymerization. The electronic, electrochemical, and optoelectronic properties varied significantly with respect to the electron-withdrawing ability and backbone planarity of the D−A copolymers. We observed reductions in E_g upon increasing the electron withdrawing strength of the acceptor moieties via strong orbital interactions. The copolymers exhibited a wide range of optical band gaps (1−1.8 eV) upon varying the nature of the acceptor units. The field-effect mobility of holes ranged from 1.1×10^{-3} cm^2 V^{-1} s^{-1} in **PTPTTP** to 8.1×10^{-3} cm^2 V^{-1} s^{-1} in **PTPTTQT**. PCEs of higher than 4.2% for photovoltaic cells fabricated from **PTPTQ**, **PTPTBT**, and **PTPTDPP** blended with $PC_{71}BM$ are obtained. It is evident that the electronic and optical properties of TPT-based D/A copolymers can be manipulated readily through variation of the acceptor strength. Our results demonstrate that designing materials with balance in the properties of bandgap, the absorption coefficient of the absorption band, and the HOMO/LUMO energy levels is a plausible pathway toward high-performance OPV application.

Acknowledgment. We thank the Ministry of Economic Affairs, Taiwan, for financial support.

Supporting Information Available: AFM images (PDF). This material is available free of charge via the Internet at http://pubs.acs.org.